

1 Estimation of sulfuric acid concentration using ambient ion 2 composition and concentration data obtained by Atmospheric 3 Pressure interface Time-of-Flight ion mass spectrometer

4 Lisa J. Beck¹, Siegfried Schobesberger², Mikko Sipilä¹, Veli-Matti Kerminen^{1,4} and Markku
5 Kulmala^{1,3,4,5}

6 ¹Institute for Atmospheric and Earth System Research/Physics, University of Helsinki, 00014 Helsinki, Finland

7 ²Department of Applied Physics, University of Eastern Finland, 70211 Kuopio, Finland

8 ³Aerosol and Haze Laboratory, Beijing Advanced Innovation Center for Soft Matter Sciences and Engineering,
9 Beijing University of Chemical Technology (BUCT), Beijing, China

10 ⁴Joint International Research Laboratory of Atmospheric and Earth System Sciences, School of Atmospheric
11 Sciences, Nanjing University, Nanjing, China

12 ⁵Faculty of Geography, Lomonosov Moscow State University, Moscow, Russia

13
14 *Correspondence to:* Lisa Beck (lisa.beck@helsinki.fi) and Markku Kulmala (markku.kulmala@helsinki.fi)

16 **Abstract**

17 Sulfuric acid (H₂SO₄, SA) is the key compound in atmospheric new particle formation. Therefore, it is crucial to
18 observe its concentration with sensitive instrumentation, such as chemical ionisation (CI) inlets coupled to
19 Atmospheric Pressure interface Time-of-Flight mass spectrometers (APi-TOF). However, there are environmental
20 conditions and physical reasons when chemical ionisation cannot be used, for example in certain remote places
21 or flight measurements with limitations regarding chemicals. Here, we propose a theoretical method to estimate
22 the SA concentration based on ambient ion composition and concentration measurements that are achieved by
23 APi-TOF alone. We derive a theoretical expression to estimate SA concentration and validate it with accurate CI-
24 APi-TOF observations. Our validation shows that the developed estimate works well during daytime in the boreal
25 forest ($R^2 = 0.85$), however it underestimates the SA concentration in e.g. Antarctic atmosphere during new
26 particle formation events where the dominating pathway for nucleation involves sulfuric acid and a base ($R^2 =$
27 0.48).

30 **1 Introduction**

31 Sulfuric acid (H₂SO₄, SA) is the key compound in atmospheric new particle formation (e.g. Weber et al., 1995,
32 1996; Birmili et al., 2003; Kulmala et al., 2004; Kuang et al., 2008; Kerminen et al., 2010; Wang et al., 2011;
33 Kulmala et al., 2014; Yao et al., 2018; Cai et al., 2021), therefore it is crucial to have accurate observations of its
34 concentration. However, ambient concentrations of H₂SO₄ are low, commonly less than a part per trillion by
35 volume ($\sim 2 \cdot 10^7$ molecules cm⁻³), making it challenging to measure it. During the recent years there have been
36 instrumental developments towards a reliable detection of H₂SO₄ in the atmosphere, particularly via the
37 development of a Chemical Ionisation Atmospheric Pressure interface Time-of-Flight mass spectrometer (CI-

38 APi-TOF, Jokinen et al., 2012), using nitric acid as a reagent ion. Still, the measurement technique with CI-API-
39 TOF is relatively challenging, as a thorough calibration i.e. with sulfuric acid as proposed by Kürten et al. (2012),
40 is needed in order to get reliable numbers. Furthermore, the loss of sulfuric acid to surfaces, such as an inlet, and
41 the correct flow rates must be known and characterised.

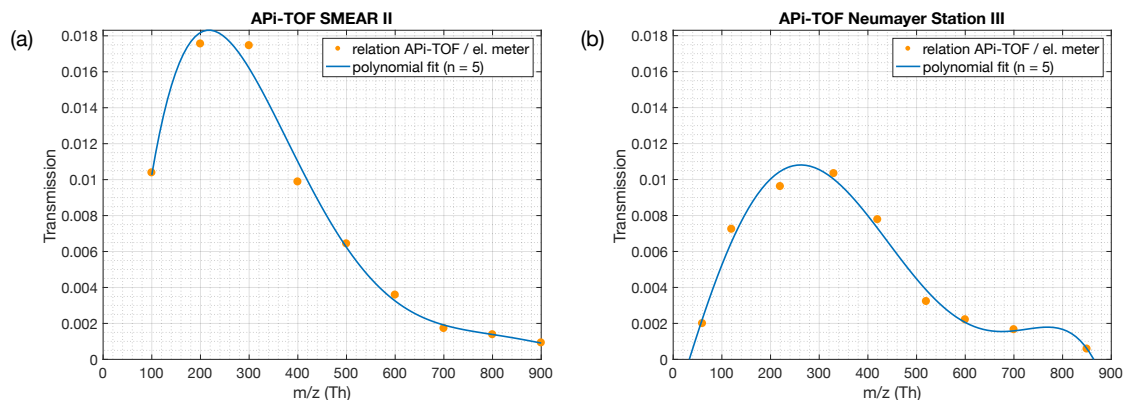
42
43 During the past decade, Atmospheric Pressure interface Time-of-Flight mass spectrometers (APi-TOF, Junninen
44 et al., 2010) have been deployed in several measurement campaigns where the use of a CI inlet was either not
45 possible or desired. In these instances, the APi-TOF only observed the composition and concentration of ambient
46 ions. The APi-TOF is capable of directly sampling and detecting naturally charged gas-phase ions, including
47 molecular clusters, and is often being used to detect clustering processes as a first step of new particle formation
48 on a molecular basis (e.g. Schobesberger et al., 2013; Jokinen et al., 2018; Beck et al., 2021). While a CI-API-
49 TOF at best has a limit of detection of around $\sim 10^4$ molecules cm^{-3} (\sim ppq level), the APi-TOF can detect
50 approximately 1% of the ambient ion concentration (Fig. 1, Junninen et al., 2010). With an average ion
51 concentration of $\sim 1000 \text{ cm}^{-3}$ per polarity (Hirsikko et al., 2011), the APi-TOF is measuring $10 \text{ ions cm}^{-3}\text{s}^{-1}$ with a
52 limit of detection of ~ 0.01 counts per second, hence 0.1 ions cm^{-3} . This corresponds to approximately a pps level
53 ($100 \cdot 10^{-21}$), showing that the limit of detection of an APi-TOF in comparison to a CI-API-TOF is lower by five
54 orders of magnitudes.

55
56 A detailed description of the APi-TOF can be found in Junninen et al. (2010). Since concentrations of neutral
57 clusters are below the detection limit of CI-API-TOF in many atmospheric conditions and environments, using
58 the APi-TOF is currently the only way to directly detect atmospheric clustering. Therefore, if we can estimate
59 H_2SO_4 concentration particularly during initial steps of new particle formation, based on the same dataset, we can
60 readily get better insight into the process itself.

61
62 Since there are only limited long term observations of H_2SO_4 concentrations, several proxies on this concentration
63 have been developed (e.g. Petäjä et al., 2009; Mikkonen et al., 2011; Lu et al., 2019; Dada et al., 2020). These
64 proxies attempt to approximate the ambient H_2SO_4 concentrations using more readily measured quantities, in
65 particular the sulfur dioxide concentration, (UV) radiation intensity and pre-existing particle number size
66 distribution that can be used to calculate the condensation sink for gas-phase H_2SO_4 . In circumstances where the
67 required data for H_2SO_4 proxies are not available, but measurements with an APi-TOF were conducted, the H_2SO_4
68 concentration can be obtained from the ion mass spectra. A first attempt of estimating the sulfuric acid
69 concentration via the concentration of atmospheric ions was introduced by Arnold and Fabian (1980), followed
70 by Eisele (1989) under the assumption that most H_2SO_4 molecules are charged by reacting with NO_3^- .

71
72 Motivated by the reasonings outlined above, we derive here an expression to estimate H_2SO_4 concentration based
73 primarily on APi-TOF observations and validate it.

74
75
76



77

78

79

80

81

82

83

84

85 2 Theoretical estimation of sulfuric acid concentration with bisulphate ion and H₂SO₄ clusters

86

87

88

89

90

91

92

93

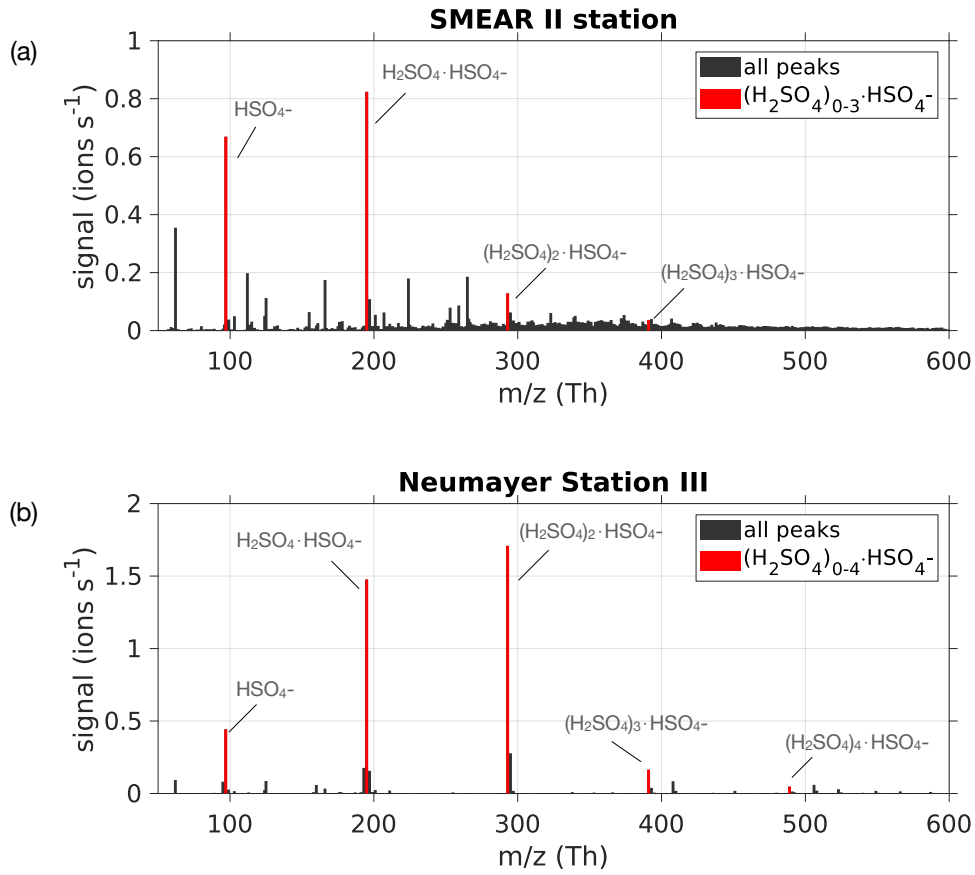
94

95

96

Figure 1 Ion transmission of the API-TOFs used in this study. The transmission efficiency was determined via production of charged particles with a NiCr wire. The concentration of the size selected ions with a Hermann nano differential mobility analyser (HDMA, Hermann, 2000) were measured with an electrometer and an APi-TOF in parallel. A more detailed description can be found in Junninen et al. (2010). Panel (a) shows the transmission efficiency of the API-TOF used for measurements at the SMEAR II Station, Hyytiälä, Finland. Panel (b) shows the transmission efficiency used for measurements at the Neumayer Station III.

Ambient ion mass spectra have usually clear evidence of gas-phase H₂SO₄, predominantly in the form of bisulphate ion (HSO₄⁻) and its adducts involving H₂SO₄, forming so-called dimers (H₂SO₄·HSO₄⁻) as well as larger clusters (Ehn et al., 2010). These ions are due to the efficient scavenging of a negative charge by ambient H₂SO₄ via proton donation, and due to the high stability of the sulfuric acid-bisulphate ion clusters, in particular for the dimer (Ortega et al., 2014). In order to estimate the sulfuric acid concentration (H₂SO₄) using measured naturally charged ions (see Fig. 2), we approximate this concentration by following the bisulphate ion HSO₄⁻, herein denoted SA_{monomer}, the dimer cluster H₂SO₄·HSO₄⁻ (SA_{dimer}) and trimer cluster (H₂SO₄)₂·HSO₄⁻ (SA_{trimer}). Any other H₂SO₄-containing ion clusters, in particular those larger than the SA_{trimer}, typically occur at much smaller concentrations and will be neglected here.



97

98 **Figure 2** (a) Mass spectrum from 50 to 600 Th measured with the API-TOF on 24 May 2017 during the time period 08:00 –
 99 18:00 (local time) at SMEAR II station, Hyytiälä, Finland. (b) Mass spectrum from 14 January 2019 between 08:00 and 18:00
 100 (local time) at Neumayer Station III, Antarctica during a new particle formation event. The bisulphate ion HSO_4^- and H_2SO_4
 101 clusters containing it were used for the estimation of H_2SO_4 concentration, and are coloured in red.

102

103

104 If we assume that the concentration of $\text{SA}_{\text{monomer}}$ depends generally on its production rate (P_1) and that its loss is
 105 by condensation onto aerosol particles (condensation sink, CS), to the SA_{dimer} when clustering with another H_2SO_4
 106 molecule, and to ion-ion recombination with positive ions (N_{pos}), we get the following equation for the $\text{SA}_{\text{monomer}}$
 107 concentration:

108

$$\frac{d[\text{SA}_{\text{monomer}}]}{dt} = P_1 - \text{CS} \cdot [\text{SA}_{\text{monomer}}] - P_2 - \alpha \cdot [\text{SA}_{\text{monomer}}] \cdot N_{\text{pos}}, \quad (1)$$

109

110 where $P_2 = k_1 \times [\text{SA}_{\text{monomer}}] \times [\text{H}_2\text{SO}_4]$ is the dimer production rate due to $\text{SA}_{\text{monomer}}\text{-H}_2\text{SO}_4$ collisions, α (≈ 1.6
 111 $\times 10^{-6} \text{ cm}^3 \text{ s}^{-1}$) is the ion-ion recombination coefficient (Kontkanen et al., 2013), and the collision rate k_1 is assumed
 112 to be constant.

113

114 For the dimer concentration we consider the production P_2 , the loss due to CS, the clustering of the SA_{dimer} with
 115 H_2SO_4 with a rate constant k_2 , and the ion-ion recombination:
 116

$$\frac{d[SA_{dimer}]}{dt} = P_2 - CS \cdot [SA_{dimer}] - k_2 \cdot [SA_{dimer}] \cdot [H_2SO_4] - \alpha \cdot [SA_{dimer}] \cdot N_{pos}, \quad (2)$$

117
 118 And with substituting P_2 , eq. 2 for SA_{dimer} changes to:
 119

$$\frac{d[SA_{dimer}]}{dt} = k_1 \cdot [SA_{monomer}] \cdot [H_2SO_4] - CS \cdot [SA_{dimer}] - k_2 \cdot [SA_{dimer}] \cdot [H_2SO_4] - \alpha \cdot [SA_{dimer}] \cdot N_{pos}. \quad (3)$$

120
 121 Finally, to produce SA_{trimer} we consider the collision of the SA_{dimer} with H_2SO_4 and the loss to the CS and ion-ion
 122 recombination. For the sake of completeness, we would additionally have to consider the loss of $SA_{trimers}$ to form
 123 the tetramer $(H_2SO_4)_3 \cdot HSO_4$, however this additional term is rather small and will therefore be neglected in this
 124 derivation. Therefore, we get the simplified equation for SA_{trimer} :
 125

$$\frac{d[SA_{trimer}]}{dt} = k_2 \cdot [SA_{dimer}] \cdot [H_2SO_4] - CS \cdot [SA_{trimer}] - \alpha \cdot [SA_{trimer}] \cdot N_{pos}. \quad (4)$$

126
 127 For simplification, we consider a pseudo-steady state condition for both dimers and trimers by setting the left-
 128 hand side of eqs. (3) and (4) to be zero, which is justified when the dimer and trimer concentrations change at
 129 rates smaller than their overall production and loss rates. Thereby, from eq. (3) we obtain:
 130

$$k_1 \cdot [SA_{monomer}] \cdot [H_2SO_4] = CS \cdot [SA_{dimer}] + k_2 \cdot [SA_{dimer}] \cdot [H_2SO_4] + \alpha \cdot [SA_{dimer}] \cdot N_{pos} \quad (5)$$

131
 132 and from eq. (4) we obtain:
 133

$$k_2 \cdot [SA_{dimer}] \cdot [H_2SO_4] = CS \cdot [SA_{trimer}] + \alpha \cdot [SA_{trimer}] \cdot N_{pos}. \quad (6)$$

134
 135 If we now deploy equation (6) in equation (5) and solve for H_2SO_4 , the result is:
 136

$$k_1 \cdot [SA_{monomer}] \cdot [H_2SO_4] = CS \cdot [SA_{dimer}] + CS \cdot [SA_{trimer}] + \alpha \cdot [SA_{dimer}] \cdot N_{pos} + \alpha \cdot [SA_{trimer}] \cdot N_{pos}, \quad (7)$$

$$[H_2SO_4] = \frac{(CS + \alpha \cdot N_{pos}) \cdot ([SA_{dimer}] + [SA_{trimer}])}{k_1 \cdot [SA_{monomer}]} \quad (8)$$

137

138 Besides the steady-state assumption, it should be noted that in deriving eq. 8 monomers, dimers and trimers were
139 assumed to have the same loss rate (CS) onto pre-existing aerosol particles. This causes an additional, yet minor,
140 uncertainty in the estimated H₂SO₄ concentrations, as such loss rates are dependent on the size/mass of the clusters
141 (e.g. Lehtinen et al., 2007; Tuovinen et al., 2021). According to Tuovinen et al. (2021), the CS of H₂SO₄ clusters
142 decreases with increasing number of H₂SO₄ molecules. The study shows that the CS of the SA_{dimer} clustered with
143 ammonia decreases to 68% (compared to one H₂SO₄ molecule) and for SA_{pentamer} with four ammonia molecules
144 to 42%. However, the order of magnitude of the CS remains the same, and the effect on the estimation of the
145 H₂SO₄ concentration is assumed to be negligible. Additionally, the CS for ions is higher than for neutral
146 compounds. The enhancement of CS has shown to reach a maximum value of 2 when the pre-existing particles
147 are < 10 nm and decreases to 1 when the pre-existing particles are > 100 nm, as shown by Mahfouz and Donahue
148 (2021). The impact of ions on CS and estimated SA concentrations depends thereby on the environmental
149 conditions determining the size distribution and charges of the pre-existing particle population. Neglecting the
150 size-dependency of CS between the SA monomers, dimers and trimers causes additional errors in estimated SA
151 concentrations; however, it is difficult to determine this effect in ambient measurements having limited data and
152 instrumentation.

153
154 Furthermore, the derivation neglects the losses of SA_{trimer} to the SA_{tetramer} and larger clusters, as well as the
155 clustering of sulfuric acid ion clusters with water and base molecules, such as NH₃. Those simplifications can
156 cause an underestimation of the H₂SO₄ concentration with the presented method. If necessary, the method can
157 easily be adapted, and bigger clusters can be included in the equation.

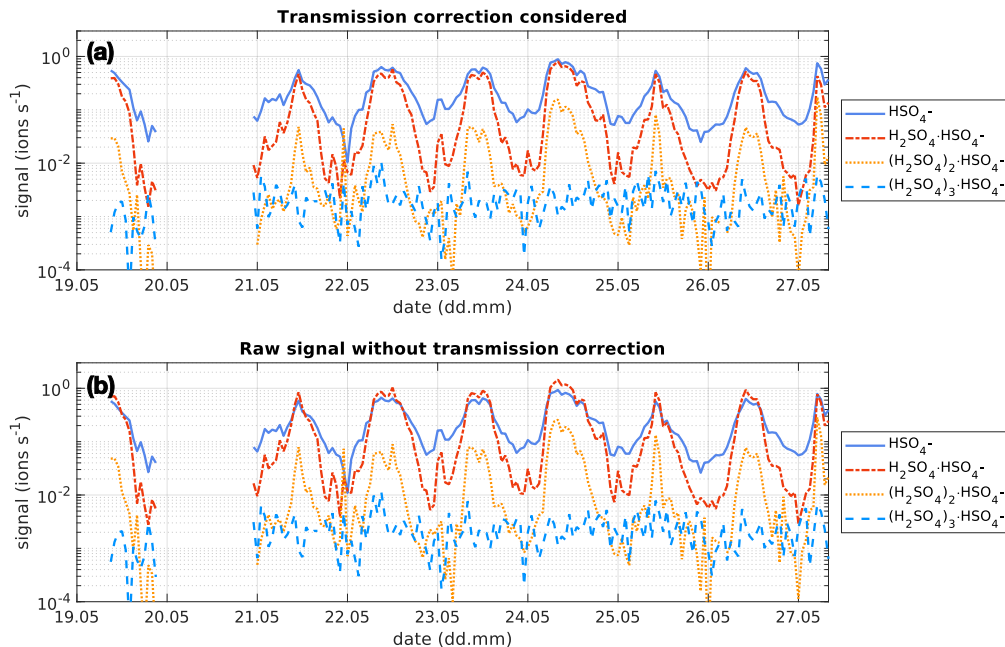
158
159 From equation 8 we also see that the concentration of H₂SO₄ is proportional to relative concentrations of sulfuric
160 acid monomers, dimers and trimers clustered with the bisulphate ion:

$$[H_2SO_4] \sim \frac{[SA_{dimer}] + [SA_{trimer}]}{[SA_{monomer}]} \quad (9)$$

162
163 To estimate the H₂SO₄ concentration with the ion mode APi-TOF, we can therefore use this theoretical approach,
164 in particular Eq. 8. For the collision rate of H₂SO₄ with HSO₄⁻ we use $k_1 = 2 \cdot 10^{-9} \text{ cm}^3 \text{ molecule}^{-1} \text{ s}^{-1}$ as in Lovejoy
165 et al. (2004). The value of CS is calculated based on Kulmala et al. (2012). Even if the CS was unknown due, for
166 example, to the lack of particle measurements, the daytime variability of the H₂SO₄ concentration could still be
167 estimated by using the relation of the H₂SO₄-containing cluster with HSO₄⁻, as it is proportional to the H₂SO₄
168 concentration (see eq. 9). If the concentration of positive small ions is not available, it can be assumed to be in the
169 range of 500 – 1000 cm⁻³ which is a reasonable approximation for the average concentration (Hirsikko et al.,
170 2011).

171
172 As the transmission of clusters within an APi-TOF depends on the tuning of the instrument and on the pressures
173 within its chambers, the transmission efficiency needs to be considered, in order to get reliable concentrations of
174 the SA_{monomer}, SA_{dimer}, and SA_{trimer}. Fig. 1 shows the transmission efficiency curve of the APi-TOF used at the
175 SMEAR II station and Neumayer Station III. The effect of applying the transmission correction to the different

176 SA clusters is depicted in Fig. 3 for the time series at the SMEAR II station. All ion signals were normalised to a
 177 transmission of 1%. As can be determined from Fig. 1a, the SA_{monomer} 's transmission at SMEAR II was $\sim 1\%$,
 178 while the dimer and trimer were corrected by a factor of $1/1.8$ and $1/1.65$, respectively. The correction was also
 179 applied on the ions measured at the Neumayer Station III according to the APi-TOF's transmission (Fig. 1b).
 180



181
 182 **Figure 3** Time series of the bisulphate ion (HSO_4^- , SA_{monomer}), H_2SO_4 clustered with bisulphate ($H_2SO_4 \cdot HSO_4^-$, SA_{dimer}), two
 183 H_2SO_4 molecules clustered with the bisulphate ion ($(H_2SO_4)_2 \cdot HSO_4^-$, SA_{trimer}) and three H_2SO_4 molecules clustered with the
 184 bisulphate ion ($(H_2SO_4)_3 \cdot HSO_4^-$, SA_{tetramer}) between 19 and 27 May 2017 at SMEAR II station, Hyytiälä, Finland. The
 185 concentration is given in ions s^{-1} as measured by the APi-TOF. The upper panel shows the concentration of the clusters
 186 considering the transmission efficiency of the instrument (see Fig. 1). The lower panel shows the concentration of the clusters
 187 without that correction and assuming a constant transmission efficiency of 1% for all ions.
 188

189 3 Validation

191 We tested the expression derived above using a dataset collected during inter-comparison measurements at the
 192 SMEAR II station in Hyytiälä, Finland (Hari and Kulmala, 2005). In Fig. 4 we show the time series of the observed
 193 H_2SO_4 concentrations, measured with a CI-APi-TOF. The CI-APi-TOF was calibrated for sulfuric acid, based on
 194 the method by Kürten et al., (2012) and resulted in a calibration factor of 2.5×10^9 . Additionally, we show the
 195 estimated sulfuric acid concentration based on APi-TOF measurements together with Eq. 8 and the sulfuric acid
 196 proxy concentration (Dada et al., 2020). The concentration of positive ions for the estimated sulfuric acid
 197 concentration was obtained from a Neutral cluster and Air Ion Spectrometer (NAIS, Airel Ltd., Mirme and Mirme,
 198 2013).

199
 200 The estimated H_2SO_4 concentration agrees with the measured one during most of the daytime. Between 06:00 and
 201 18:00 local time, the correlation (R^2) between the estimated and measured H_2SO_4 concentration is equal to 0.85

202 with a root mean square error (RMSE) of $4.12 \times 10^5 \text{ cm}^{-3}$. During night-time, the corresponding values are 0.85
 203 and $3.23 \times 10^5 \text{ cm}^{-3}$ (Table 1).

204

205 The scatter plot in Fig. 5 shows that the estimated H_2SO_4 concentrations agree well with the observed one when
 206 H_2SO_4 concentrations are larger than $2 \times 10^6 \text{ cm}^{-3}$, demonstrating that our method works particularly well at the
 207 SMEAR II station during conditions that favour the formation of H_2SO_4 -containing clusters.

208

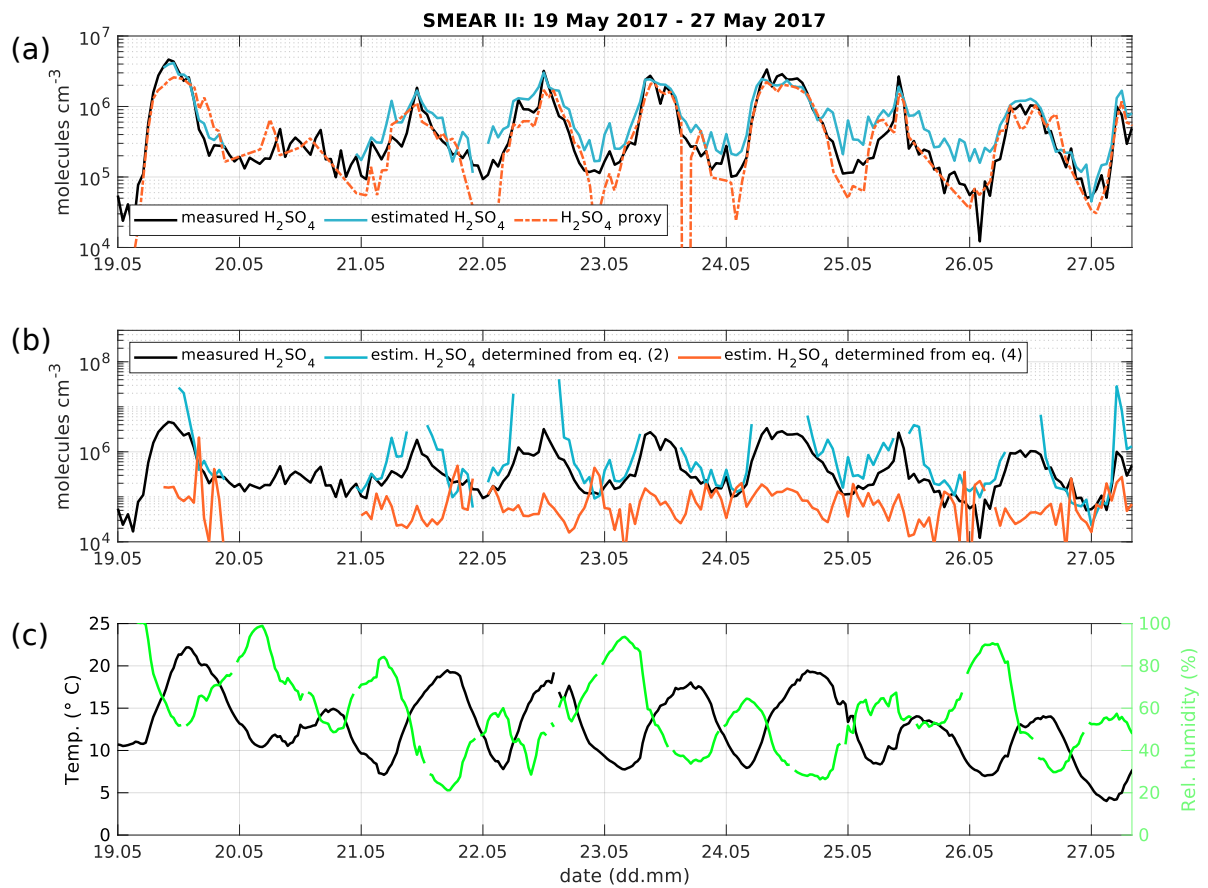
209

210 **Table 1:** Root mean square error (RMSE) and R^2 of the estimated H_2SO_4 concentration at the SMEAR II station and Neumayer
 211 Station III. The day- and night-time are split in 06:00 – 18:00 local time (LT) and 18:00 – 06:00 LT, respectively. For the
 212 SMEAR II station, we also show the RMSE and R^2 of the H_2SO_4 proxy calculated with the introduced method by (Dada et al.,
 213 2020).

	Root mean square error (RMSE)		
	SMEAR II		Neumayer Station III
	Estimated H_2SO_4 eq. (8)	H_2SO_4 proxy	Estimated H_2SO_4 eq. (8)
Daytime	$4.12 \times 10^5 \text{ cm}^{-3}$	$5.54 \times 10^5 \text{ cm}^{-3}$	$1.43 \times 10^6 \text{ cm}^{-3}$
Night-time	$3.23 \times 10^5 \text{ cm}^{-3}$	$4.25 \times 10^5 \text{ cm}^{-3}$	$1.63 \times 10^6 \text{ cm}^{-3}$
	R^2		
Daytime	0.85	0.78	0.48
Night-time	0.85	0.84	0.37

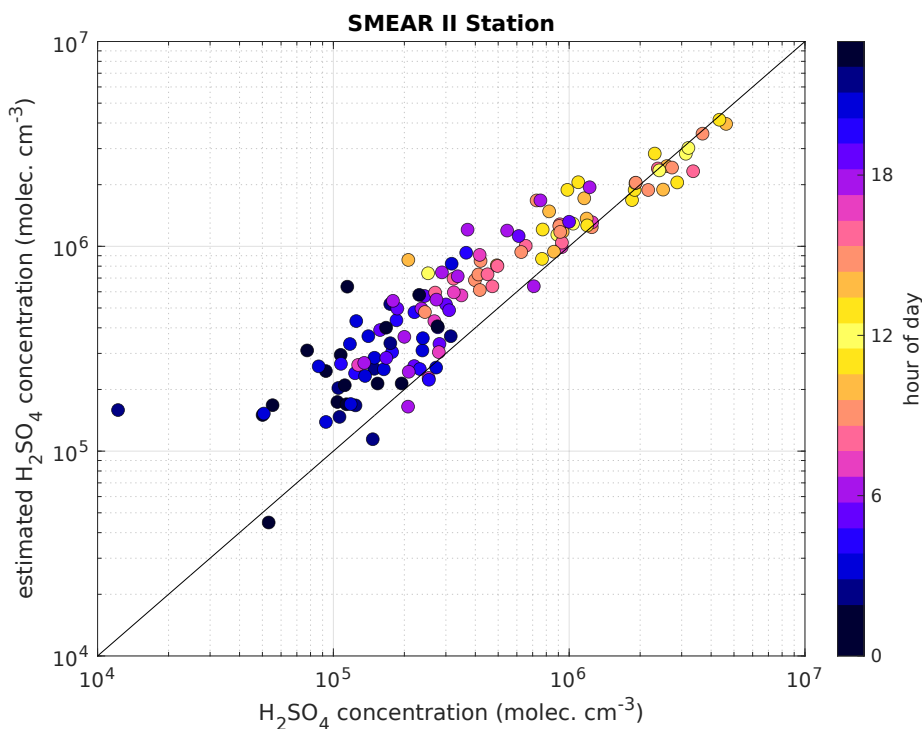
214

215



216
 217
 218
 219
 220
 221

Figure 4 (a) Time series of measured H_2SO_4 concentration from the CI-API-TOF (black) and estimated H_2SO_4 concentration from the API-TOF (blue) and H_2SO_4 proxy from Dada et al. (2020) (orange) between 19 and 27 May 2017. The concentration is given in molecules cm^{-3} . (b) Measured H_2SO_4 concentration as in panel (a) in black and determined concentration from eq. 2 (blue) and eq. 4 (orange). (c) Temperature and relative humidity.

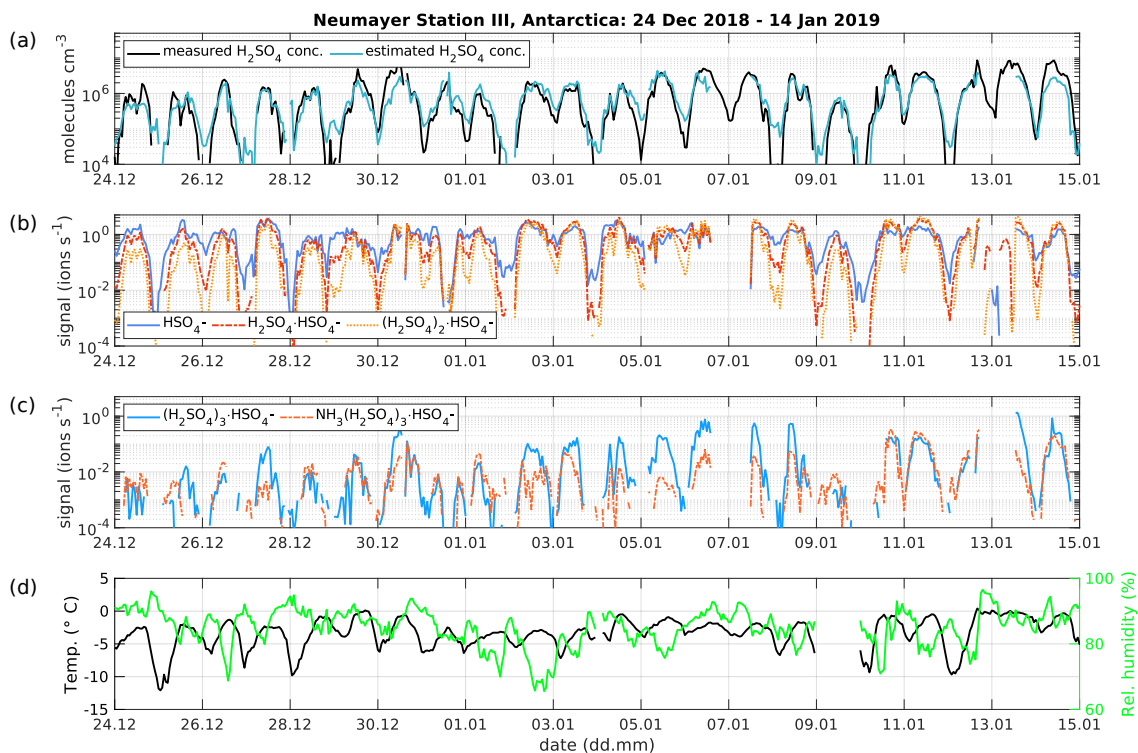


222
 223 **Figure 5** Measured H₂SO₄ concentration using a CI-APi-TOF (horizontal-axis) versus estimated H₂SO₄ concentration based
 224 on APi-TOF results (vertical-axis) at SMEAR II station. For the estimation of H₂SO₄, the transmission efficiency was taken
 225 into account. The colour is indicating the hour of the day and the black line is the 1:1 ratio. Between 08:00 and 16:00 local
 226 time, the concentrations are agreeing well. The shown data contains the time period from 19 to 27 May 2017. The overall
 227 correlation coefficient (Pearson) is 0.94.

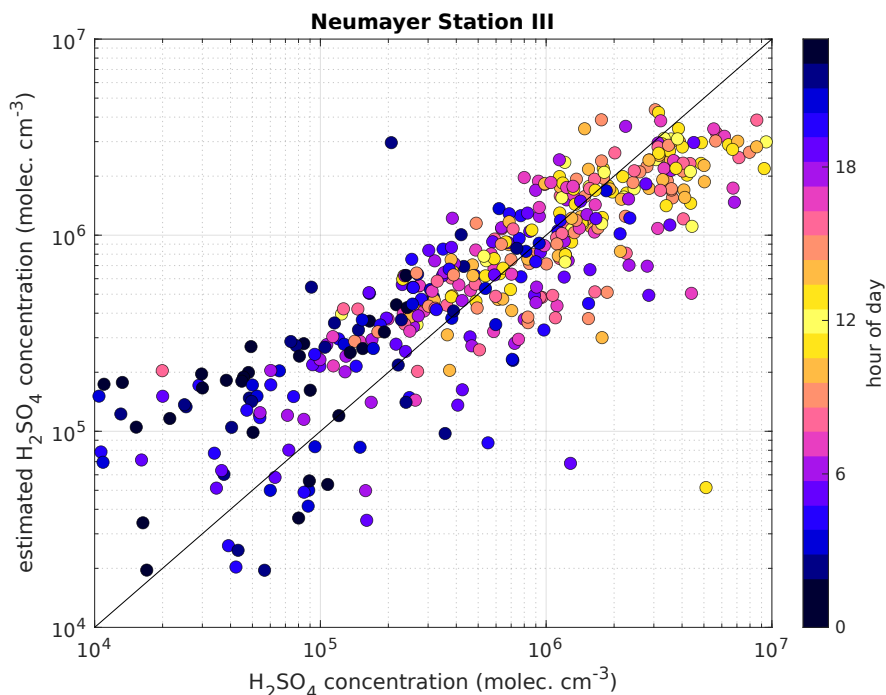
228
 229 For the sake of completeness, the estimation of the H₂SO₄ concentration determined from Eqs. 2 and 4, assuming
 230 pseudo-steady state, are depicted in Fig. 4b. The estimated H₂SO₄ concentration from Eq. 2 is overestimating,
 231 while solving Eq. 4 for H₂SO₄ is underestimating the real concentration as those equations are only
 232 approximations. By combining the various approximations, Eq. 8 yields in the best fit to the observed SA
 233 concentration.

234
 235 The presented method was also applied to measurements taken at the Neumayer Station III, Antarctica, in order
 236 to test it in a different environment. Here, we used the condensation sink reported by Weller et al. (2015) at
 237 Neumayer Station of $1 \times 10^{-3} \text{ s}^{-1}$. Figure 6 shows a three-week period between 24 December 2018 and 14 January
 238 2019. The calibration factor of the CI-APi-TOF used for measuring the sulfuric acid concentration is 4.9×10^9 .
 239 Here, the estimated sulfuric acid concentration underestimates the measured concentration when the SA_{tetramer} and
 240 NH₃(H₂SO₄)₃HSO₄⁻ cluster show high concentrations (Fig. 6c). A possible explanation for the underestimation
 241 might be the neglect of the growth of sulfuric acid to oligomers larger than the tetramer, as well as its clustering
 242 with bases and water (Fig. 6b and c). In coastal Antarctica, the main nucleating mechanism was observed to be
 243 negative ion-induced sulfuric acid-ammonia nucleation, acting as a major sink for sulfuric acid molecules due to
 244 its clustering with bases (Jokinen et al., 2018). Including the SA_{tetramer} and SA_{tetramer} clustered with NH₃ in the
 245 estimation equation improved the correlation (R²) from 0.48 to 0.54. Furthermore, as mentioned above, the value
 246 of CS for Neumayer was assumed to be constant (10^{-3} s^{-1}) due to the lack of data needed for its calculation. This

247 simplification certainly causes additional errors in estimated SA concentrations, especially during periods of high
 248 sea salt concentrations causing potentially large variations in values of CS. Nevertheless, the diurnal variation of
 249 the SA concentration is represented well by this method. During times with lower sulfuric acid concentrations,
 250 our method gives higher values than the measured concentrations (Fig. 6).



251
 252 **Figure 6** (a) Time series of measured H_2SO_4 concentration from the CI-API-TOF (black) and estimated H_2SO_4 concentration
 253 from the API-TOF (blue) between 24 December 2018 and 14 January 2019 at Neumayer Station III, Antarctica. The
 254 concentration is given in molecules cm^{-3} . (b) Time series of the bisulphate ion (HSO_4^- , $\text{SA}_{\text{monomer}}$), H_2SO_4 clustered with
 255 bisulphate ($\text{H}_2\text{SO}_4 \cdot \text{HSO}_4^-$, SA_{dimer}), two H_2SO_4 molecules clustered with the bisulphate ion ($(\text{H}_2\text{SO}_4)_2 \cdot \text{HSO}_4^-$, $\text{SA}_{\text{trimer}}$) and (c)
 256 three H_2SO_4 molecules clustered with the bisulphate ion ($(\text{H}_2\text{SO}_4)_3 \cdot \text{HSO}_4^-$, $\text{SA}_{\text{tetramer}}$) as well as the $\text{SA}_{\text{tetramer}}$ clustered with
 257 NH_3 . (d) Temperature and relative humidity measured at Neumayer Station III.
 258



259
 260 **Figure 7** Measured H₂SO₄ concentration using a CI-APi-TOF (horizontal axis) versus estimated H₂SO₄ concentration based
 261 on APi-TOF results (vertical axis) at the Neumayer Station III. For the estimation of H₂SO₄, the transmission efficiency was
 262 taken into account. The colour is indicating the hour of the day and the black line is the 1:1 ratio. The shown data contains the
 263 time period from 24 December 2016 to 14 January 2019. The overall correlation coefficient (Pearson) is 0.77.
 264
 265

266 4 Conclusions

267 Here we derived a theoretical expression to estimate H₂SO₄ concentrations based on APi-TOF measurements of
 268 ambient ions. The estimation agrees well with the measured concentration during daytime in the boreal forest (R²
 269 = 0.85), indicating that the estimation is able to represent the diurnal variation and trend of H₂SO₄ concentrations
 270 during most of the time when active clustering of sulfuric acid is inducing the initial step(s) of atmospheric new
 271 particle formation. However, in an atmosphere, where sulfuric acid is the dominating pathway for initiating new
 272 particle formation, the method might underestimate the H₂SO₄ concentrations, as this method does not include the
 273 rapid clustering to bigger of sulfuric acid clusters and clustering with bases directly, e.g. in the Antarctic
 274 atmosphere (R² = 0.48; during daytime).
 275

276 The APi-TOF's "ion mode", i.e. direct ion sampling without chemical ionisation, remains a crucial tool in many
 277 field deployments and laboratory studies, since it is extremely sensitive and allows for observing atmospheric
 278 clustering molecule by molecule, which in most cases is impossible when relying on chemical ionization.
 279 Therefore, having available a reliable estimate of H₂SO₄ concentration allows us to utilise the APi-TOF ion mode
 280 even more effectively.
 281

283 Data availability

284 The data can be accessed via Zenodo (10.5281/zenodo.5266313).

285

286 **Author contribution**

287 LJB, SS, VMK and MK designed the study. LJB and MS performed the measurements. SS and LJB derived the
288 equations. LJB processed and analysed the data and performed the data visualisation. MK and VMK supervised
289 the process. All authors commented and edited the paper.

290

291 **Competing interests**

292 The authors declare that they have no conflict of interest.

293

294 **Acknowledgements**

295 We acknowledge the following projects: ACCC Flagship funded by the Academy of Finland grant number
296 337549, Academy professorship funded by the Academy of Finland (grant no. 302958), Academy of Finland
297 projects no. 1325656, 310682, 316114, 325647 and 296628 , Russian Mega Grant project “Megapolis - heat and
298 pollution island: interdisciplinary hydroclimatic, geochemical and ecological analysis” application reference
299 2020-220-08-5835, “Quantifying carbon sink, CarbonSink+ and their interaction with air quality” INAR project
300 funded by Jane and Aatos Erkkö Foundation, European Research Council (ERC) project ATM-GTP Contract No.
301 742206 and GASPARCON, grant agreement no. 714621. We thank the tofTools team for providing the tools for
302 the mass spectrometry analysis. We thank the technical and scientific staff in Hyytiälä SMEAR II and the
303 technicians and scientists of the Neumayer overwintering teams of the years 2018 and 2019. We thank Lubna
304 Dada for calculating the SA proxy for SMEAR II station. We thank Janne Lampilahti for providing the codes to
305 process the NAIS dataset.

306 **References**

- 307 Arnold, F. and Fabian, R.: First measurements of gas phase sulphuric acid in the stratosphere, 283, 55–57,
308 <https://doi.org/10.1038/283055a0>, 1980.
- 309 Beck, L. J., Sarnela, N., Junninen, H., Hoppe, C. J. M., Garmash, O., Bianchi, F., Riva, M., Rose, C., Peräkylä,
310 O., Wimmer, D., Kausiala, O., Jokinen, T., Ahonen, L., Mikkilä, J., Hakala, J., He, X.-C., Kontkanen, J., Wolf,
311 K. K. E., Cappelletti, D., Mazzola, M., Traversi, R., Petroselli, C., Viola, A. P., Vitale, V., Lange, R., Massling,
312 A., Nøjgaard, J. K., Krejci, R., Karlsson, L., Zieger, P., Jang, S., Lee, K., Vakkari, V., Lampilahti, J., Thakur, R.
313 C., Leino, K., Kangasluoma, J., Duplissy, E.-M., Siivola, E., Marbouti, M., Tham, Y. J., Saiz-Lopez, A., Petäjä,
314 T., Ehn, M., Worsnop, D. R., Skov, H., Kulmala, M., Kerminen, V.-M., and Sipilä, M.: Differing Mechanisms
315 of New Particle Formation at Two Arctic Sites, *Geophysical Research Letters*, 48,
316 <https://doi.org/10.1029/2020GL091334>, 2021.
- 317 Birmili, W., Berresheim, H., Plass-Dülmer, C., Elste, T., Gilge, S., Wiedensohler, A., and Uhrner, U.: The
318 Hohenpeissenberg aerosol formation experiment (HAFEX): a long-term study including size-resolved aerosol,
319 H₂SO₄, OH, and monoterpenes measurements, 3, 361–376, <https://doi.org/10.5194/acp-3-361-2003>, 2003.
- 320 Cai, R., Yan, C., Yang, D., Yin, R., Lu, Y., Deng, C., Fu, Y., Ruan, J., Li, X., Kontkanen, J., Zhang, Q.,
321 Kangasluoma, J., Ma, Y., Hao, J., Worsnop, D. R., Bianchi, F., Paasonen, P., Kerminen, V.-M., Liu, Y., Wang,
322 L., Zheng, J., Kulmala, M., and Jiang, J.: Sulfuric acid–amine nucleation in urban Beijing, 21, 2457–2468,
323 <https://doi.org/10.5194/acp-21-2457-2021>, 2021.
- 324 Dada, L., Ylivinkka, I., Baalbaki, R., Li, C., Guo, Y., Yan, C., Yao, L., Sarnela, N., Jokinen, T., Daellenbach, K.
325 R., Yin, R., Deng, C., Chu, B., Nieminen, T., Wang, Y., Lin, Z., Thakur, R. C., Kontkanen, J., Stolzenburg, D.,
326 Sipilä, M., Hussein, T., Paasonen, P., Bianchi, F., Salma, I., Weidinger, T., Pikridas, M., Sciare, J., Jiang, J.,
327 Liu, Y., Petäjä, T., Kerminen, V.-M., and Kulmala, M.: Sources and sinks driving sulfuric acid concentrations in
328 contrasting environments: implications on proxy calculations, 20, 11747–11766, [https://doi.org/10.5194/acp-20-](https://doi.org/10.5194/acp-20-11747-2020)
329 [11747-2020](https://doi.org/10.5194/acp-20-11747-2020), 2020.
- 330 Ehn, M., Junninen, H., Petäjä, T., Kurtén, T., Kerminen, V.-M., Schobesberger, S., Manninen, H. E., Ortega, I.
331 K., Vehkamäki, H., Kulmala, M., and Worsnop, D. R.: Composition and temporal behavior of ambient ions in
332 the boreal forest, 10, 8513–8530, <https://doi.org/10.5194/acp-10-8513-2010>, 2010.
- 333 Eisele, F. L.: Natural and anthropogenic negative ions in the troposphere, 94, 2183–2196,
334 <https://doi.org/10.1029/JD094iD02p02183>, 1989.
- 335 Hari, P. and Kulmala, M.: Station for Measuring Ecosystem–Atmosphere Relations (SMEAR II), *Bor. Env.*
336 *Res.*, 10, 315–322, 2005.
- 337 Herrmann, W., Eichler, T., Bernardo, N., and Fernandez de la Mora, J.: Turbulent transition arises at Re 35 000
338 in a short Vienna type DMA with a large laminarizing inlet, *Proceedings of the annual conference of the*
339 *AAAR*, St. Louis, MO, 6–10 October 2000.
- 340
341 Hirsikko, A., Nieminen, T., Gagné, S., Lehtipalo, K., Manninen, H. E., Ehn, M., Hörrak, U., Kerminen, V.-M.,
342 Laakso, L., McMurry, P. H., Mirme, A., Mirme, S., Petäjä, T., Tammet, H., Vakkari, V., Vana, M., and
343 Kulmala, M.: Atmospheric ions and nucleation: a review of observations, 11, 767–798,
344 <https://doi.org/10.5194/acp-11-767-2011>, 2011.
- 345 Jokinen, T., Sipilä, M., Junninen, H., Ehn, M., Lönn, G., Hakala, J., Petäjä, T., Mauldin III, R. L., Kulmala, M.,
346 and Worsnop, D. R.: Atmospheric sulphuric acid and neutral cluster measurements using CI-API-TOF, 12,
347 4117–4125, <https://doi.org/10.5194/acp-12-4117-2012>, 2012.
- 348 Jokinen, T., Sipilä, M., Kontkanen, J., Vakkari, V., Tisler, P., Duplissy, E.-M., Junninen, H., Kangasluoma, J.,
349 Manninen, H. E., Petäjä, T., Kulmala, M., Worsnop, D. R., Kirkby, J., Virkkula, A., and Kerminen, V.-M.: Ion-
350 induced sulfuric acid–ammonia nucleation drives particle formation in coastal Antarctica, *Sci Adv*, 4,
351 <https://doi.org/10.1126/sciadv.aat9744>, 2018.

- 352 Junninen, H., Ehn, M., Petäjä, T., Luosujärvi, L., Kotiaho, T., Kostianen, R., Rohner, U., Gonin, M., Fuhrer, K.,
353 Kulmala, M., and Worsnop, D. R.: A high-resolution mass spectrometer to measure atmospheric ion
354 composition, 3, 1039–1053, <https://doi.org/10.5194/amt-3-1039-2010>, 2010.
- 355 Kerminen, V.-M., Petäjä, T., Manninen, H. E., Paasonen, P., Nieminen, T., Sipilä, M., Junninen, H., Ehn, M.,
356 Gagné, S., Laakso, L., Riipinen, I., Vehkamäki, H., Kurten, T., Ortega, I. K., Dal Maso, M., Brus, D.,
357 Hyvärinen, A., Lihavainen, H., Leppä, J., Lehtinen, K. E. J., Mirme, A., Mirme, S., Hörrak, U., Berndt, T.,
358 Stratmann, F., Birmili, W., Wiedensohler, A., Metzger, A., Dommen, J., Baltensperger, U., Kiendler-Scharr, A.,
359 Mentel, T. F., Wildt, J., Winkler, P. M., Wagner, P. E., Petzold, A., Minikin, A., Plass-Dülmer, C., Pöschl, U.,
360 Laaksonen, A., and Kulmala, M.: Atmospheric nucleation: highlights of the EUCAARI project and future
361 directions, 10, 10829–10848, <https://doi.org/10.5194/acp-10-10829-2010>, 2010.
- 362 Kontkanen, J., Lehtinen, K. E. J., Nieminen, T., Manninen, H. E., Lehtipalo, K., Kerminen, V.-M., and Kulmala,
363 M.: Estimating the contribution of ion–ion recombination to sub-2 nm cluster concentrations from atmospheric
364 measurements, 13, 11391–11401, <https://doi.org/10.5194/acp-13-11391-2013>, 2013.
- 365 Kuang, C., McMurry, P. H., McCormick, A. V., and Eisele, F. L.: Dependence of nucleation rates on sulfuric
366 acid vapor concentration in diverse atmospheric locations, 113, <https://doi.org/10.1029/2007JD009253>, 2008.
- 367 Kulmala, M., Vehkamäki, H., Petäjä, T., Dal Maso, M., Lauri, A., Kerminen, V.-M., Birmili, W., and McMurry,
368 P. H.: Formation and growth rates of ultrafine atmospheric particles: a review of observations, *Journal of*
369 *Aerosol Science*, 35, 143–176, <https://doi.org/10.1016/j.jaerosci.2003.10.003>, 2004.
- 370 Kulmala, M., Petäjä, T., Nieminen, T., Sipilä, M., Manninen, H. E., Lehtipalo, K., Dal Maso, M., Aalto, P. P.,
371 Junninen, H., Paasonen, P., Riipinen, I., Lehtinen, K. E. J., Laaksonen, A., and Kerminen, V.-M.: Measurement
372 of the nucleation of atmospheric aerosol particles, 7, 1651–1667, <https://doi.org/10.1038/nprot.2012.091>, 2012.
- 373 Kulmala, M., Petäjä, T., Ehn, M., Thornton, J., Sipilä, M., Worsnop, D. R., and Kerminen, V.-M.: Chemistry of
374 Atmospheric Nucleation: On the Recent Advances on Precursor Characterization and Atmospheric Cluster
375 Composition in Connection with Atmospheric New Particle Formation, 65, 21–37,
376 <https://doi.org/10.1146/annurev-physchem-040412-110014>, 2014.
- 377 Kürten, A., Rondo, L., Ehrhart, S., and Curtius, J.: Calibration of a Chemical Ionization Mass Spectrometer for
378 the Measurement of Gaseous Sulfuric Acid, *J. Phys. Chem. A*, 116, 6375–6386,
379 <https://doi.org/10.1021/jp212123n>, 2012.
- 380 Lehtinen, K. E. J., Dal Maso, M., Kulmala, M., and Kerminen, V.-M.: Estimating nucleation rates from apparent
381 particle formation rates and vice versa: Revised formulation of the Kerminen–Kulmala equation, *Journal of*
382 *Aerosol Science*, 38, 988–994, <https://doi.org/10.1016/j.jaerosci.2007.06.009>, 2007.
- 383 Lovejoy, E. R., Curtius, J., and Froyd, K. D.: Atmospheric ion-induced nucleation of sulfuric acid and water,
384 109, <https://doi.org/10.1029/2003JD004460>, 2004.
- 385 Lu, Y., Yan, C., Fu, Y., Chen, Y., Liu, Y., Yang, G., Wang, Y., Bianchi, F., Chu, B., Zhou, Y., Yin, R.,
386 Baalbaki, R., Garmash, O., Deng, C., Wang, W., Liu, Y., Petäjä, T., Kerminen, V.-M., Jiang, J., Kulmala, M.,
387 and Wang, L.: A proxy for atmospheric daytime gaseous sulfuric acid concentration in urban Beijing, 19, 1971–
388 1983, <https://doi.org/10.5194/acp-19-1971-2019>, 2019.
- 389 Mahfouz, N. G. A. and Donahue, N. M.: Technical note: The enhancement limit of coagulation scavenging of
390 small charged particles, 21, 3827–3832, <https://doi.org/10.5194/acp-21-3827-2021>, 2021.
- 391 Mikkonen, S., Romakkaniemi, S., Smith, J. N., Korhonen, H., Petäjä, T., Plass-Duelmer, C., Boy, M., McMurry,
392 P. H., Lehtinen, K. E. J., Joutsensaari, J., Hamed, A., Mauldin III, R. L., Birmili, W., Spindler, G., Arnold, F.,
393 Kulmala, M., and Laaksonen, A.: A statistical proxy for sulphuric acid concentration, 11, 11319–11334,
394 <https://doi.org/10.5194/acp-11-11319-2011>, 2011.
- 395 Mirme, S. and Mirme, A.: The mathematical principles and design of the NAIS – a spectrometer for the
396 measurement of cluster ion and nanometer aerosol size distributions, 6, 1061–1071, <https://doi.org/10.5194/amt-6-1061-2013>, 2013.

398 Ortega, I. K., Olenius, T., Kupiainen-Määttä, O., Loukonen, V., Kurtén, T., and Vehkamäki, H.: Electrical
399 charging changes the composition of sulfuric acid–ammonia/dimethylamine clusters, 14, 7995–8007,
400 <https://doi.org/10.5194/acp-14-7995-2014>, 2014.

401 Petäjä, T., Mauldin, I. I. I., Kosciuch, E., McGrath, J., Nieminen, T., Paasonen, P., Boy, M., Adamov, A.,
402 Kotiaho, T., and Kulmala, M.: Sulfuric acid and OH concentrations in a boreal forest site, 9, 7435–7448,
403 <https://doi.org/10.5194/acp-9-7435-2009>, 2009.

404 Schobesberger, S., Junninen, H., Bianchi, F., Lönn, G., Ehn, M., Lehtipalo, K., Dommen, J., Ehrhart, S., Ortega,
405 I. K., Franchin, A., Nieminen, T., Riccobono, F., Hutterli, M., Duplissy, J., Almeida, J., Amorim, A.,
406 Breitenlechner, M., Downard, A. J., Dunne, E. M., Flagan, R. C., Kajos, M., Keskinen, H., Kirkby, J., Kupc, A.,
407 Kürten, A., Kurtén, T., Laaksonen, A., Mathot, S., Onnela, A., Praplan, A. P., Rondo, L., Santos, F. D.,
408 Schallhart, S., Schnitzhofer, R., Sipilä, M., Tomé, A., Tsagkogeorgas, G., Vehkamäki, H., Wimmer, D.,
409 Baltensperger, U., Carslaw, K. S., Curtius, J., Hansel, A., Petäjä, T., Kulmala, M., Donahue, N. M., and
410 Worsnop, D. R.: Molecular understanding of atmospheric particle formation from sulfuric acid and large
411 oxidized organic molecules, PNAS, 110, 17223–17228, <https://doi.org/10.1073/pnas.1306973110>, 2013.

412 Tuovinen, S., Kontkanen, J., Cai, R., and Kulmala, M.: Condensation sink of atmospheric vapors: the effect of
413 vapor properties and the resulting uncertainties, Environ. Sci.: Atmos., 1, 543–557,
414 <https://doi.org/10.1039/D1EA00032B>, 2021.

415 Wang, Z. B., Hu, M., Yue, D. L., Zheng, J., Zhang, R. Y., Wiedensohler, A., Wu, Z. J., Nieminen, T., and Boy,
416 M.: Evaluation on the role of sulfuric acid in the mechanisms of new particle formation for Beijing case, 11,
417 12663–12671, <https://doi.org/10.5194/acp-11-12663-2011>, 2011.

418 Weber, R. J., McMurry, P. H., Eisele, F. L., and Tanner, D. J.: Measurement of Expected Nucleation Precursor
419 Species and 3–500-nm Diameter Particles at Mauna Loa Observatory, Hawaii, 52, 2242–2257,
420 [https://doi.org/10.1175/1520-0469\(1995\)052](https://doi.org/10.1175/1520-0469(1995)052), 1995.

421 Weber, R. J., Marti, J. J., McMurry, P. H., Eisele, F. L., Tanner, D. J., and Jefferson, A.: Measured Atmospheric
422 New Particle Formation Rates: Implications for Nucleation Mechanisms, 151, 53–64,
423 <https://doi.org/10.1080/00986449608936541>, 1996.

424 Weller, R., Schmidt, K., Teinilä, K., and Hillamo, R.: Natural new particle formation at the coastal Antarctic site
425 Neumayer, 15, 11399–11410, <https://doi.org/10.5194/acp-15-11399-2015>, 2015.

426 Yao, L., Garmash, O., Bianchi, F., Zheng, J., Yan, C., Kontkanen, J., Junninen, H., Mazon, S. B., Ehn, M.,
427 Paasonen, P., Sipilä, M., Wang, M., Wang, X., Xiao, S., Chen, H., Lu, Y., Zhang, B., Wang, D., Fu, Q., Geng,
428 F., Li, L., Wang, H., Qiao, L., Yang, X., Chen, J., Kerminen, V.-M., Petäjä, T., Worsnop, D. R., Kulmala, M.,
429 and Wang, L.: Atmospheric new particle formation from sulfuric acid and amines in a Chinese megacity, 361,
430 278–281, <https://doi.org/10.1126/science.aao4839>, 2018.

431